High Purity and High Density Ti3SiC2/Al2O3 Composites Were Prepared at High Temperature

Xuye Wang
University of Jinan
Fangfang Qi
University of Jinan
Jun Ji
University of Jinan
Guopu Shi
University of Jinan
Qinggang Li
University of Jinan
Zhi Wang (wangzhi@ujn.edu.cn)
University of Jinan https://orcid.org/0000-0002-8001-6648

Research Article

Keywords: High temperature, Ti3SiC2/Al2O3 Composites, High density, Mechanical properties

DOI: https://doi.org/10.21203/rs.3.rs-77477/v1

Abstract

In this study, Ti_3SiC_2/Al_2O_3 composites were prepared via in-situ hot pressing sintering at 1550 °C. Al used as a sintering aid reduced the production of TiC impurity phase and stabilized the crystal lattice of Ti_3SiC_2 to inhibit its decomposiition at high temperature. This is because Al replaced some of the Si atoms to form $Ti_3(Si_{1-x}Al_x)C_2$, which showed a crystal structure similar to that of Ti_3SiC_2. The addition of Al is a prerequisite for the formation of high density Ti_3SiC_2/Al_2O_3 composites at high temperature. Laminar Ti_3SiC_2 grains and granular Al_2O_3 grains were densely packed and tightly bonded, furthermore, unique mosaic structure of Ti_3SiC_2-Al_2O_3 created at high temperatures improve the mechanical properties such as hardness, bending strength and fracture toughness of Ti_3SiC_2/Al_2O_3 composites, with the highest reaching 16.97 GPa, 553.38 MPa and 9.63 $MPa{\cdot}m^{1/2}$, respectively. The mechanism responsible for improved mechanical properties for Ti_3SiC_2/Al_2O_3 composites were the synergistic action of grain pullout, microcrack deflection, and extend the crack growth from two different kinds of grains.

1. Introduction

The progress and development of society can not be separated from the progress of materials. Materials as the pillar of contemporary civilization play a decisive role in various fields and have gradually become the material basis for human survival. Owing to its good stability in high temperature, high strain, corrosion, strong oxidation and other harsh conditions, ceramic materials are widely used to prepare various kinds of military and civilian materials, such as parts of automobile engines, protective appliances of armor and medical appliances [1–3]. However, owing to the interior bonding way of the ceramic material is high-energy covalent bond, which is difficult to break. Resulted in the lattice structure of ceramics are stable. The dislocation slip and deformation are hard to come into being when the ceramic material to be stressed, therefore, the ceramic materials will instantaneously rupture, it is the reason why ceramic materials are brittle [4–5]. Therefore, ceramics are mostly compounded with ductile fibers, ductile metal materials or polymer materials with excellent plasticity [6–9].

Alumina ceramics, which exhibit high hardness, high chemical stability, and suitable flexure strength, have attracted significant attention in recent years, and as a result, they have been commonly used in industry. However, their low fracture toughness limits their further development as a reliable ceramic material, therefore, the toughening and strengthening of Alumina ceramics is a research hotspot of ceramics [10–13]. The toughening of Al_2O_3 usually involves two ways: self-toughening and composite material toughening. The self-toughening means that in the process of sintering the seed of crystals is introduced within the matrix by phase transformation toughening of matrix. Composite toughening means that fiber, whisker, enhanced dispersion strengthening body, or good ductility of metal is introduced into the matrix to achieve the effect of toughening ceramic matrix. However, the above mentioned composite toughening materials still have some problems to be solved in system design and material combination.

With the development of the research, a new type of ceramic MAX phase has gradually appeared. MAX phases (M = early transition metal; A = main group element; X = C or N) [14], which were first reported by Jeitschko in the 1960s, have received considerable attention in recent years. To date, more than 150 types of MAX phases have been discovered, and their properties have been investigated [15, 16]. In the case of the 312 phase, Ti_3SiC_2, Ti_3AlC_2 and, Ti_3GeC_2 have been widely applied owing to their facile preparation and excellent stability. In this work, we continued the idea of complementing the advantages of composite materials, designed and prepared Ti_3SiC_2/Al_2O_3 ceramic composites with the main goal of improving the mechanical properties of the materials in the service environment. However, when employing an in-situ preparation at high temperature, highly pure Ti_3SiC_2/Al_2O_3 composites are challenging to obtain owing to the narrow phase area of Ti_3SiC_2, which results in the formation of TiC as an impurity.

Cai et al [17] fabricated Ti_3SiC_2/TiC-Al_2O_3 composites with different Al_2O_3 contents and believed the in-situ generated TiC to be the matrix phase. The composites showed high flexural strength. However, their fracture toughness was low. At the present stage, some researchers have realized the in-situ synthesis of Ti_3SiC_2 by adopting various methods such as thermal isostatic sintering, hot-pressed sintering, discharge plasma sintering, self-spreading sintering, and chemical vapor deposition synthesis [18–22]. Wang et al [23] used Al_2O_3, TiC, and Si as the raw materials and synthesized Ti_3SiC_2/Al_2O_3 composites via in-situ reaction using spark plasma sintering at 1300 °C. The resulting composites showed good mechanical properties, but contained a large amount of TiC impurities. Mishra et al [24] prepared Ti-Si-C series materials with high hardness (22.5 GPa) and elastoplastic deformation through self-propagating sintering with Ti, Si and C as raw materials. Zhang et al [25] used different mixing methods (vibrating sieve mixing for 24 h and mechanical alloying for 500 h) to fully mix the materials of Ti, Si and TiC with a ratio of 1:1:2, and used pulse discharge sintering at a lower temperature (1250 °C ~ 1300 °C) to prepare Ti_3SiC_2 materials. Although they have synthesized Ti_3SiC_2/Al_2O_3 composites with high purity, the composites has lower density, resulting in poor mechanical properties.

Therefore, the purpose of this study is to synthesize high density Ti_3SiC_2/Al_2O_3 composites at high temperature while ensuring the purity of Ti_3SiC_2/Al_2O_3 composites. In this study, Al was employed as a sintering additive for the synthesis of Ti_3SiC_2/Al_2O_3 composites. The optimum Al amount for improving the mechanical properties of the composites was determined. The effect of the Al content (mole percentage) on the microstructure and mechanical properties of the Ti_3SiC_2/Al_2O_3 composites was investigated. This study provides a basis for further investigate the anti-oxidation ability of Ti_3SiC_2/Al_2O_3 composites.

2. Materials And Methods

The raw materials used in the present work were pure fine powders of Al_2O_3 (99.8% pure, an average particle size of 1 μm), Ti (99.9% pure, an average particle size of 1 μm), SiC (99.8% pure, an average particle size of 800 nm), C (99.95% pure, an average particle size of 1 μm), Si (99.9% pure, an average

particle size of 1 μm) and Al (99.9% pure, an average particle size of 1 μm). The Al_2O_3:Ti_3SiC_2 volume ratio (fabricated via in-situ reaction; molar ratio of Ti:SiC:C = 3:1:1) was 6:4. Al was doped to form 3Ti/1SiC/1C/xAl mixtures, where x = 0-0.25 mol, the difference of Al content between samples was 0.05 mol. The ingredients were dispersed evenly in ethanol at a speed of 200 rpm for 4 h in planetary mill (XQM-2, China). Then the slurry was dried in the drying oven at 70 °C and sifted by a 200 mesh sifter. Thereafter, the prepared powders were sintered in vacuum hot pressing furnace (VVPgr-80-2300, China) at 1550 °C for 1.5 h under the vacuum pressure of below 8.0×10^{-3} MPa, and the pressure was kept 30 MPa under uniaxial pressure when the sintering temperature was 1550 °C. The heating rates were set as 10 °C·min^{-1} (0-1200 °C) and 5 °C·min^{-1} (1200–1550 °C). Finally, the sintered samples were taken out when cooled naturally to room temperature in the furnace.

The irregularity on the surfaces of the obtained samples were gradually grinded by SiC power and polished with abrasive paper. The specimens used for measuring the flexural strength and fracture toughness were processed into long columns with the dimensions of 36 mm × 4 mm × 3 mm and 36 mm × 4 mm × 2 mm, respectively; the chamfering was 0.5 mm. All simples must be cleaned by ultrasonic cleaning in the ethanol solution for 20 min for removal of pollutants. Then the flexural strength and fracture toughness were measured through three-point bending method by electromechanical universal testing machine (CMT5504, MTSSYSTEMS, China) with cross-head speed of 0.5 mm/min and span of 30 mm. The relative density of samples was tested through Archimedes method by density balance at room temperature. Vickers hardness tester (HV-1000IS, China) was used to determine the micro-hardness with the applying load of 1Kg for 20 s, each final value was averaged over six measurements. The phase compositions of those samples was judged by X-ray diffraction (D8 ADVANCE, Bruker) with Cu K radition, Microstructure investigations was performed by scanning electron microscopy (SEM, FEIQUANTA FEG 250, United States) equipped with an energy dispersive spectroscopy (EDS) on prepared cross-sections after spraying gold for 20 s. The microstructures and nanoscale lattice spacings of the samples were examined using transmission electron microscopy (TEM) (Tecnai G2 F20, USA).

3. Results

3.1 Phase compositions

Figure 1 shows the XRD patterns of the samples with different Al contents. It can be seen that all samples consist mainly of three crystalline phases, namely Al_2O_3, Ti_3SiC_2 (major phase) and TiC (secondary phase). No other crystalline phases could be identified from the patterns. However, phase ratio of the sample synthesized with different Al contents were different, the phase compositions was calculated approximately using the K value method:

$$W_x = I_{xi} / \sum_{i=A}^{N} \frac{I_i}{K_A^i}$$

where W_x is the mass faction of the X phase, Ixi represents the highest peak value of the X phase, and K^i_A can determined via RIR. The results of refinement are shown in Fig. 2. It can be seen that the production of Ti_3SiC_2 is small in the sample without Al. At the Al content of 0.05 and 0.15 mol, the intensity of Ti_3SiC_2 diffraction peak decreased significantly and the TiC content increased sharply. At this time, the introduction of Al had a negative impact on the synthesis of Ti_3SiC_2 phase. The fundamental reason is that due to the narrow Ti_3SiC_2 phase zone, its stoichiometric ratio and thermodynamic conditions tend to be out of balance. The new diffraction peak of Ti_3SiC_2 appears at 37.10 after the addition of Al increases further. When the Al content is 0.2 mol, an obvious diffraction peak of Ti_3SiC_2 appears near 39.58, and the Ti_3SiC_2 content reaches the maximum of 37.6 vol.%.

The magnified view of the diffraction peak corresponding to Ti_3SiC_2 observed at 39.667° (right hand side of Fig. 1) shows that the position of the diffraction peak shifted to the left. This implies an increase in the interplanar distance [26]. The radius and lattice spacing of Al atoms are larger than those of Si atoms. This indicates that some of the Si atoms were replaced by Al atoms. This was confirmed by calculating the lattice spacing of the sample with 0.2 mol Al using TEM. The microstructural features of the sample with 0.2 mol Al were examined using TEM, as shown in Fig. 3. The distance between the (0 0 1) crystal planes of Ti_3SiC_2, obtained by calibrating the lattice fringes, was 1.7680 nm, which matches well with the standard value (1.7630 nm). This indicates that the formation of the solid solution of Al and Si increased the lattice spacing of Ti_3SiC_2 while maintaining the crystal structure of Ti_3SiC_2. This corresponds to the left shift of the diffraction peak in the XRD patterns.

3.2 Microstructure

Figure 4 shows the micrographs and elemental composition of the fracture surface of the sample without Al obtained using EDS. It could be observed that there was an obvious generation of long columnar grains in the sample, whose size was 2 ~ 3 μm. Combined with the study of Ti_3SiC_2/Al_2O_3 composites and the XRD analysis results, it was believed that the long columnar grains were Ti_3SiC_2. Furthermore, it could be seen from the sectional element distribution diagram that the purple area of Si enrichment appeared in the local area of Ti_3SiC_2 grains. Hence, the mole ratio of Ti_3SiC_2 was unbalanced. This may be the reason for the low Ti_3SiC_2 content. The result was also consistent with the XRD pattern.

Figure 5 shows the fracture surface of sample with different Al content. As can be seen, there were still some gaps and pores of the sample without Al. Ti_3SiC_2 grains and Al_2O_3 grains were not closely combined, and the densification degree of the sample needed to be further improved. This might be due to the difference of thermal expansion coefficient, which produced internal stress during the cooling process and causes the tiny crack along the grain boundary. Although a small amount of liquid phase had been involved in the sintering process of Ti_3SiC_2/Al_2O_3 composites, the advantages of promoting sintering were not obvious.

With the introduction of Al, the gaps and pores between grains gradually disappeared and the grains growth well. The molten Al had a good wetting effect on Al_2O_3 and Ti_3SiC_2 grains, which could promote sintering. In addition, with no abnormal growth of Al_2O_3 and Ti_3SiC_2 grains being observed. Compared with the average particle size of Al_2O_3 in the raw material powder (1um), the sintered Al_2O_3 grains size still remained small. When the content of Al was too much, obvious liquid phase could be observed (as shown in Fig. 5d). Although liquid phase sintering contributes to the densification of the material, excessive molten Al adversely affects the mechanical properties of the composites.

3.3 Mechanical properties

Figure 6 showed the actual density and relative density of Ti_3SiC_2/Al_2O_3 composites with different Al contents. The actual density of the material had a slight tendency to decrease, but the overall change was not significant. Considering that the density of Al was less than other raw materials, the introduction of Al theoretically reduced the actual density of Ti_3SiC_2/Al_2O_3 composites. The relative density of each group of samples exceeds 98.5%, which fully indicates that high temperature is conducive to densification and sintering of Ti_3SiC_2/Al_2O_3 composites, and its relative density generally showed an increasing trend, indicating that the densification of samples increased with the introduction of Al.

The vickers hardness, bending strength and fracture toughness of samples were shown in Fig. 7. The mechanical properties of the Ti_3SiC_2/Al_2O_3 composites had been significantly improved with the increase of Al content. The hardness of the samples first increased with an increase in the Al content, reached the maximum values at the Al content of 0.2 mol, and then decreased with a further increase in the Al content (beyond 0.2 mol). The increasing hardness of Ti_3SiC_2/Al_2O_3 composites was mainly correlated with the increasing densification degree of materials. At the beginning, the hardness of the sample was significantly improved for two reasons: first, there was a large amount of TiC in the sample. Figure 8 shows the micrographs and elemental composition of the fracture surface of the sample with 0.05 mol Al obtained using EDS, it could be observed that there were concentrated Ti and C elements in local areas in the sample. Combined with the results of XRD analysis, it could be concluded that there are scattered TiC particles in the cross section. The high hardness of TiC was conducive to the Ti_3SiC_2/Al_2O_3 composites to maintain a good hardness in the compression process. At the same time, the introduction of Al had a certain role in promoting densification of Ti_3SiC_2/Al_2O_3 composites sintered. When Al adding quantity was too much, the advantage of the hardness improved became significantly lower, but finally did not appear to reduce the hardness of samples, combined with the section on the material microstructure and the analysis of the relative density, hardness could be thought of improving also depended on the internal structure of Ti_3SiC_2/Al_2O_3 composites density.

With the increase of Al content, the flexural strength of Ti_3SiC_2/Al_2O_3 composite material showed a trend of increasing firstly, then the flexural strength reduced when the Al adding exceed 0.15 mol. The reason why the bending strength had a trend of reducing included two aspects. On the one hand, the purity of Ti_3SiC_2 is the major factor affecting the flexural strength. On the other hand, the grain boundary of the material existed more molten phase. Although liquid phase sintering contributes to the densification of

the material, excessive molten Al adversely affects the mechanical properties of the composites. The presence of too many brittle amorphous phases at the interface reduces the intergranular interface bonding strength. Under the action of an external stress field, cracks develop rapidly along the interface with weak bonding, reducing the advantage of liquid phase sintering. It could be observed that the fracture toughness of the sample with 0.05 mol Al contents was decreased. Compared with the results of phase analysis of Ti_3SiC_2/Al_2O_3 composites in the previous section, it was believed that the decrease of Ti_3SiC_2 content was the main cause of the decrease of fracture toughness. The fracture toughness of the samples increased with an increase in the Al content and reached the maximum value of 9.63 $MPa{\cdot}m^{1/2}$ at 0.2 mol Al.

4. Discussions

4.1 Densification mechanism of Ti_3SiC_2/Al_2O_3 composites

Figure 5(c) shows the SEM micrographs of the fracture surfaces of the sample with 0.2 mol Al contents. It could be observed that the interfaces between Ti_3SiC_2 and Al_2O_3 is relatively smooth, the close combination between them reflected the good densification and sintering of Ti_3SiC_2/Al_2O_3 composites. The continuous improvement of the densification degree of Ti_3SiC_2/Al_2O_3 composites were mainly strong driving force of sintering at high temperature. Furthermore, The mass transfer of liquid phase formed by Al melting at high temperature generates viscous flow under the action of sintering pressure, and the diffusion rate of atoms was greatly improved. The solid solution would occur between Al and Si before reaching the Si melting point, further reducing the temperature of the liquid phase. With the continuous diffusion of the liquid phase to the surrounding, the cracks between the particles in the sintered samples were gradually filled by the melt, which promoted the densification of Ti_3SiC_2/Al_2O_3 composites.

4.2 Strengthening mechanism of mechanical properties

High resolution transmission electron microscope (HRTEM) photographs of Ti_3SiC_2 and Al_2O_3 interfaces were shown in Fig. 9. According to the calibration of its crystal stripe, the left side was Ti_3SiC_2 (104) plane, and the spacing between adjacent crystal faces was 0.2812 nm. By comparing the crystal lattice spacing of Ti_3SiC_2 (104) plane in Ti_3SiC_2 standard card (0.2769 nm), it could be seen that the solid solution of Al at Si position increased the spacing between crystal faces of Ti_3SiC_2, but still basically maintained the crystal structure of Ti_3SiC_2 itself. This corresponded to the phenomenon that the diffraction peak of Ti_3SiC_2 was shifted to a small Angle in the above X-ray diffraction results. The (113) and (012) planes of Al_2O_3 could be obtained by calibrating the lattice fringe on the right side. Furthermore, the interface between Ti_3SiC_2 and Al_2O_3 was clear, and there was no obvious amorphous phase at the interface, which showed good interface stability and it was conducive to the improvement of mechanical properties of Ti_3SiC_2/Al_2O_3 composite.

Figure 10 showed the distribution of elements of the sample doped with 0.25 mol Ge. Obvious step-shaped structure could be observed in the figure. By comparison with EDS elemental surface analysis results, it could be seen that the step-shaped pattern in Fig. 10(a) mainly came from Ti_3SiC_2 phase, and the step-shaped pattern in Fig. 10(b) mainly came from Al_2O_3 phase. At this time, the lamellar structure in Ti_3SiC_2/Al_2O_3 composite material existed not only because of the crystal structure of Ti_3SiC_2 itself, but also because of the fracture stress of Al_2O_3 particles. Both of these two phases had a step-shaped pattern, which made Ti_3SiC_2 and Al_2O_3 not only showed the traditional intercrystalline fracture mode when subjected to external stress, but also had the characteristics of obviously passing through the laminar fracture. Therefore, more fracture energy could be absorbed to deflect the crack. In addition, the interlacing of Ti_3SiC_2 grains effectively prevented the crack growth [27–29], thus improving the mechanical properties of Ti_3SiC_2/Al_2O_3 composites. Previous studies had shown that the content of Ti_3SiC_2 in the system was significantly correlated with the mechanical properties of Ti_3SiC_2/Al_2O_3 composites, and the increase of Ti_3SiC_2 volume fraction often led to the improvement of material strength and mechanical properties.

Figure 11 shows the SEM micrographs of the fracture surfaces of the sample with 0.2 mol Al contents. The pits resulted from small Al_2O_3 grain's pullout were found in the fractured surfaces of Ti_3SiC_2 grains (marked as white arrows in Fig. 11(a)). Al_2O_3 particles themselves belong to intergranular fracture, but under high sintering driving force, their grains are embedded in Ti_3SiC_2 grains, The small Al_2O_3 grains inclined to be pulled out (marked as white circle in Fig. 11(a)). Figure 11(b) is the SEM micrographs of Ti_3SiC_2 grains embedded with large grain Al_2O_3 grains. The red arrows represent the direction of the crack. Ti_3SiC_2 grains themselves belong to transgranular fracture, As the crack travels through the Ti_3SiC_2 grains and encounters large Al_2O_3 grains, it will be deflected again along the Al_2O_3 grains, which will greatly improve the fracture toughness of the Ti_3SiC_2/Al_2O_3 composites.

5. Conclusions

In this study, high density Ti_3SiC_2/Al_2O_3 composites were synthesized by Al doping at high temperature, furthermore, ensure the purity of Ti_3SiC_2/Al_2O_3 composites as much as possible. the influence of Al content on the microstructure and mechanical performances on Ti_3SiC_2/Al_2O_3 composites prepared was studied. The conclusions of this present paper could be summarized as follows:

(1) Introduction of Al could reduce the production of TiC impurity phase and stabilize the crystal lattice of Ti_3SiC_2 to promote its formation. Ti_3SiC_2/Al_2O_3 composites synthesized in-situ had the highest content of Ti_3SiC_2 (37.6 vol.%)when 0.2 mol Al content.

(2) Under the action of molten Al and the driving force of high temperature sintering, the Ti_3SiC_2/Al_2O_3 composites achieved densification sintering with a relative density of 99.6%.

(3) Unique mosaic structure of Ti_3SiC_2-Al_2O_3 created at high temperatures could improve the mechanical properties of the Ti_3SiC_2/Al_2O_3 composites by extend the crack growth path and grain pullout.

6. Declarations

Acknowledgements

This study was financially supported by the National Natural Science Foundation of China under grant no. 51872118 and the Natural Science Foundation of Shandong Province under grant no. ZR2019MEM055.

7. References

1. Li K, Wang DL, Chen H, et al. Normalized evaluation of thermal shock resistance for ceramic materials. J Adv Ceram 2014, 3: 250-258.
2. Mohamed AS, Elayaperumal A. Experimental investigation on the effect of ceramic coating on engine performance and emission characteristics for cleaner production. J Clean Prod 2019, 214: 506-513.
3. Samaei SM, Gato-Trinidad S, Altaee A. The Application of Pressure-Driven Ceramic Membrane Technology for the Treatment of Industrial Wastewaters-A Review. Sep Purif Technol 2018, 200: 198-220.
4. Jiang DY. Recent progresses in the phenomenological description for the indentation size effect in microhardness testing of brittle ceramics. J Adv Ceram 2012, 1: 38-49.
5. Verma AS, Kumar D, Dubey AK. A review of an innovative concept to increase the toughness of the ceramics by piezoelectric secondary phases. Ceram Int 2018, 44: 16119-16127.
6. Yunus DE, He R, Shi WT, et al. Short fiber reinforced 3d printed ceramic composite with shear induced alignment. Ceram Int 2018, 43: 11766-11772.
7. Wu N, Xue FD, Wang JY, et al. Effect of TiN addition on the microstructure and mechanical properties of TiB2-FeNi based cermets. Mat Sci Eng A-Struct 2019, 743: 546-557.
8. Zhao GL, Huang CZ, Liu HL, et al. Preparation of in-situ growth TaC whiskers toughening Al2O3 ceramic matrix composite. Int J Refract Met H 2013, 36: 122-125.
9. Wang JY, Yang ZH, Duan XM, et al. Microstructure and mechanical properties of SiCf/SiBCN ceramic matrix composites. J Adv Ceram 2015, 4: 31-38.
10. Zhang ZF, Li L, Yang JC, γ-Al2O3 thin film formation via oxidation of b-NiAl (1 1 0). Acta Mater 2011, 59: 5905-5916.
11. Du JS, Tang BH, Liu W, et al. Effects of annealing and firing in wet hydrogen on the dielectric breakdown strengths of alumina ceramics. J Adv Ceram 2020, 9: 173-182.

12. Gao CK, Yan JY, Dong L, et al. Influence of Al2O3, layer thickness on high-temperature stability of TiAlN-Al2O3. Appl Surf Sci 2013, 285: 287-292.
13. Du JS, Tang BH, Liu W, et al. Effects of annealing and firing in wet hydrogen on the dielectric breakdown strengths of alumina ceramics. J Adv Ceram 2020, 9: 173-182.
14. Zheng Z, Lim SH, Lai DMY, et al. Probing the oxidation behavior of Ti2AlC MAX phase powders between 200 and 1000 °C. J Eur Ceram Soc 2017, 37: 43-51.
15. Xu Q, Zhou YC, Zhang HM, et al. Theoretical prediction, synthesis, and crystal structure determination of new MAX phase compound V2SnC. J Adv Ceram 2020, 9: 481-492.
16. Radovic M, Barsoum MW, El-Raghy T, et al. Effect of temperature strain rate and grain size on the mechanical response of Ti3SiC2 in tension. Acta Mater 2002, 50: 1297-1306.
17. Cai YZ, Yin HF, Pan LP, et al. Microstructures and mechanical properties of Ti3SiC2/TiC-Al2O3 composites synthesized by reactive hot pressing. Mat Sci Eng A-Struct 2013, 571: 137-143.
18. Jiang XS, Liu WX, Li JR, et al. Microstructures and mechanical properties of Cu/Ti3SiC2/C/MWCNTs composites prepared by vacuum hot-pressing sintering. J Alloys Compd 2015, 618: 700-706.
19. Turki F, Abderrazak H, Schoenstein F, et al. Physico-chemical and mechanical properties of Ti3SiC2-based materials elaborated from SiC/Ti by reactive spark plasma sintering. J Adv Ceram 2019, 8: 47-61.
20. Eklund P, Murugaiah A, Emmerlich J, et al. Homoepitaxial growth of Ti-Si-C MAX-phase thin films on bulk Ti3SiC2 substrates. J Crystal Growth 2007, 304: 264-269.
21. Barsoum MW, ElRaghy P. Synthesis and characterization of a remarkable ceramic: Ti3SiC2. J Am Ceram Soc 1996, 79: 1953-1956.
22. Yang DX, Zhou Y, Yan XH, et al. Highly conductive wear resistant Cu/Ti3SiC2(TiC/SiC) co-continuous composites via vacuum infiltration process. J Adv Ceram 2020, 9: 83-93.
23. Wang HJ, Jin ZH, Miyamoto Y. Ti3SiC2/Al2O3 composites prepared by SPS. Ceram. Int 2003, 29: 539-542.
24. Mishra SK, Khusboo, Sherbakov VA. Fabrication of in-situ Ti-Si-C fine grained composite by the self propagating high temperature synthesis (SHS) process. Int J of Refract Met H 2011, 29: 209-213.
25. Zhang ZF, Sun ZM, Hashimoto H, et al. Fabrication and microstructure characterization of Ti3SiC2 synthesized from Ti/Si/2TiC powders using the pulse discharge sintering (PDS) technique. J Am Ceram Soc 2003, 86: 431-436.
26. Qi, FF, Shi GP, Xu K, et al. Microstructure and mechanical properties of hot pressed Ti3SiC2/Al2O3. Ceram Int 2019, 45: 11099-11104.
27. Xu HQ, Zhang L, Wang Z, et al. Effects of Ta2O5 on mechanical properties and elements diffusion of Ti/Al2O3 composites prepared via hot pressing sintering. Ceram Int 2017, 43: 7935-7941.
28. Zawrah MF, Aly MH. In-situ formation of Al2O3-SiC-mullite from Al-matrix composites. Ceram Int 2006, 32: 21-28.

29. Liu JW, Zhou XB, Tatarko P, et al. Fabrication, microstructure, and properties of SiC/Al4SiC4 multiphase ceramics via an in-situ formed liquid phase sintering. J Adv Ceram 2020, 9: 193-203.

Figures

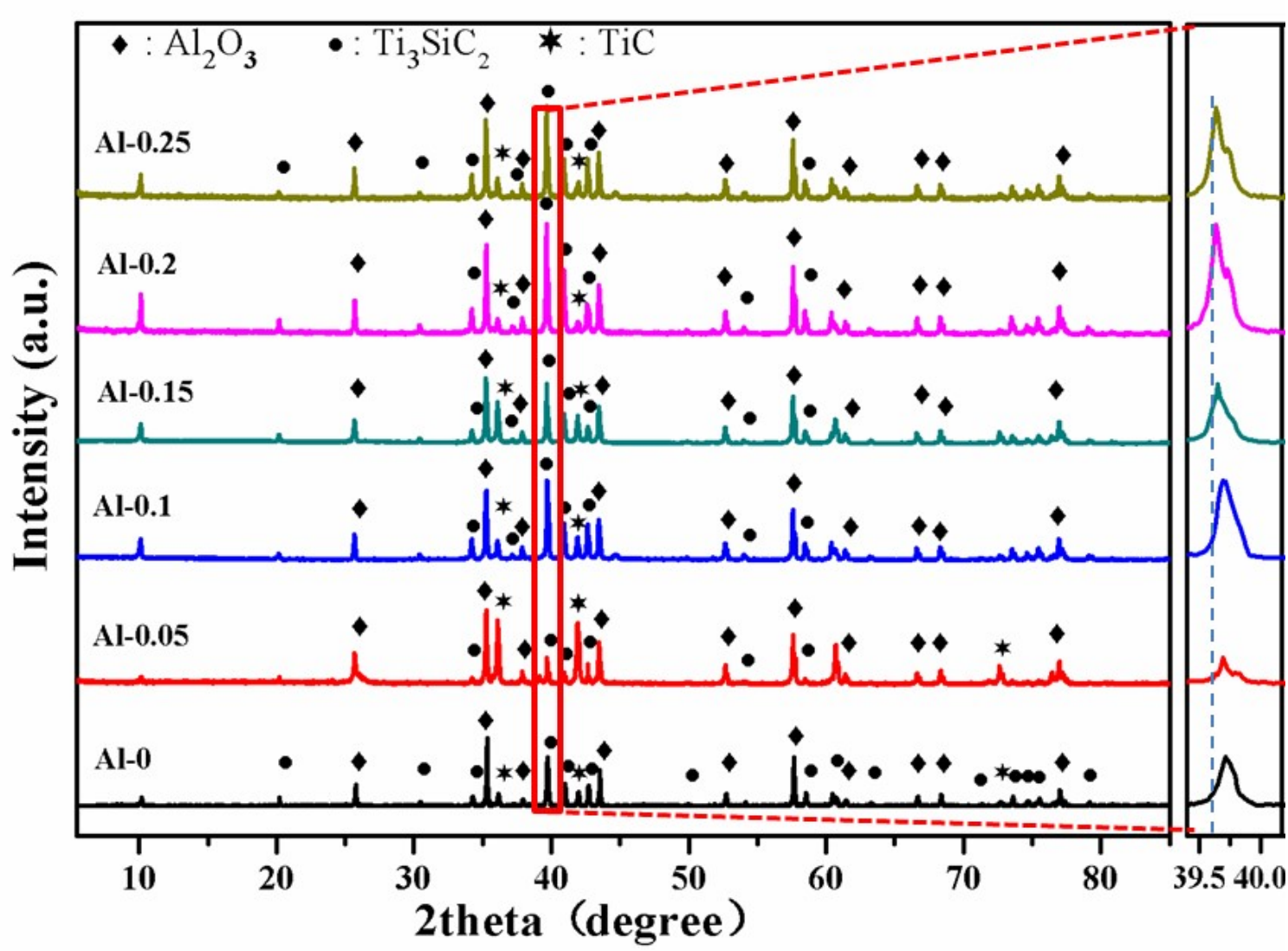

Figure 1

XRD patterns of the Ti3SiC2/Al2O3 composites with different Al contents.

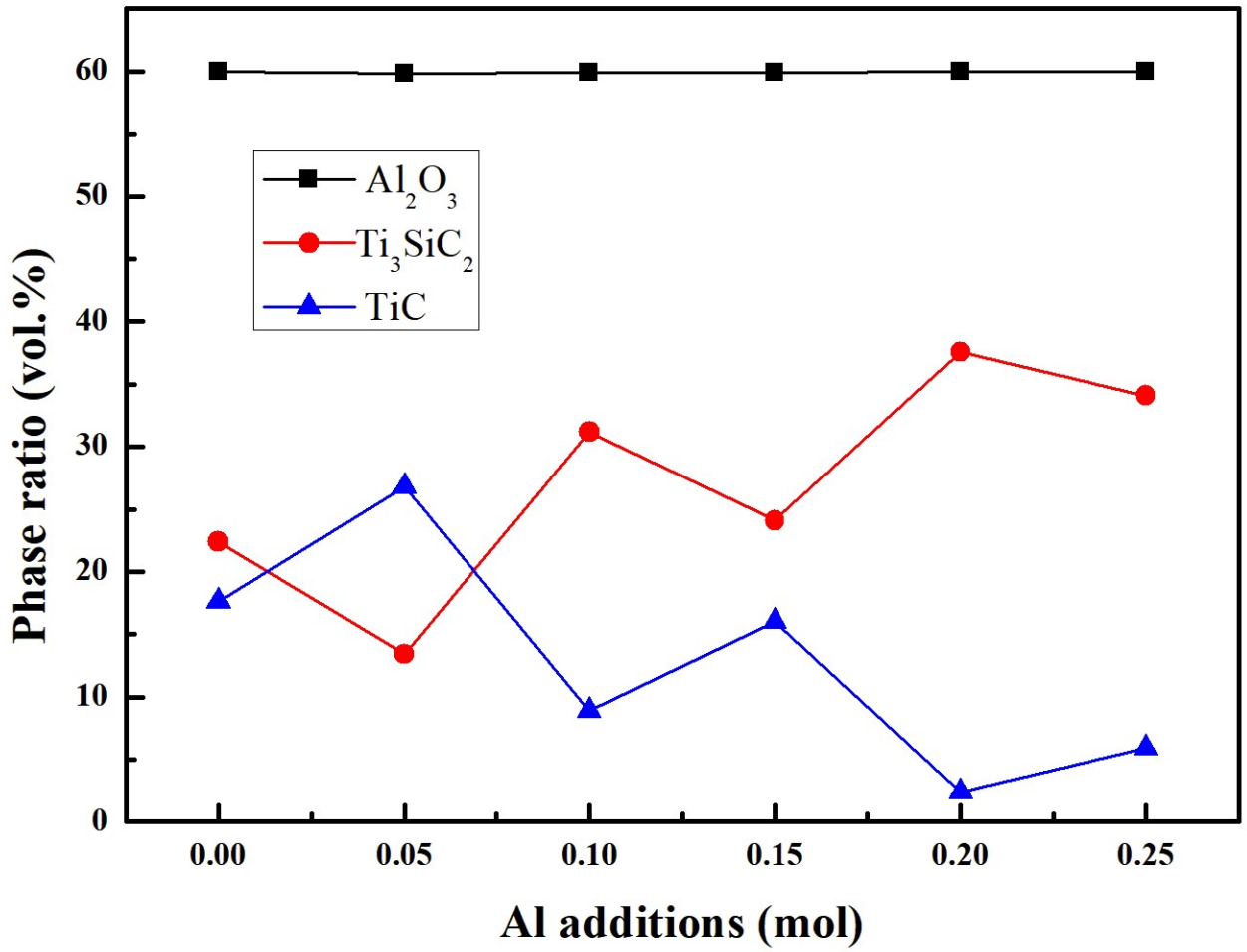

Figure 2

Phase ratio of the Ti3SiC2/Al2O3 composites with different Al contents.

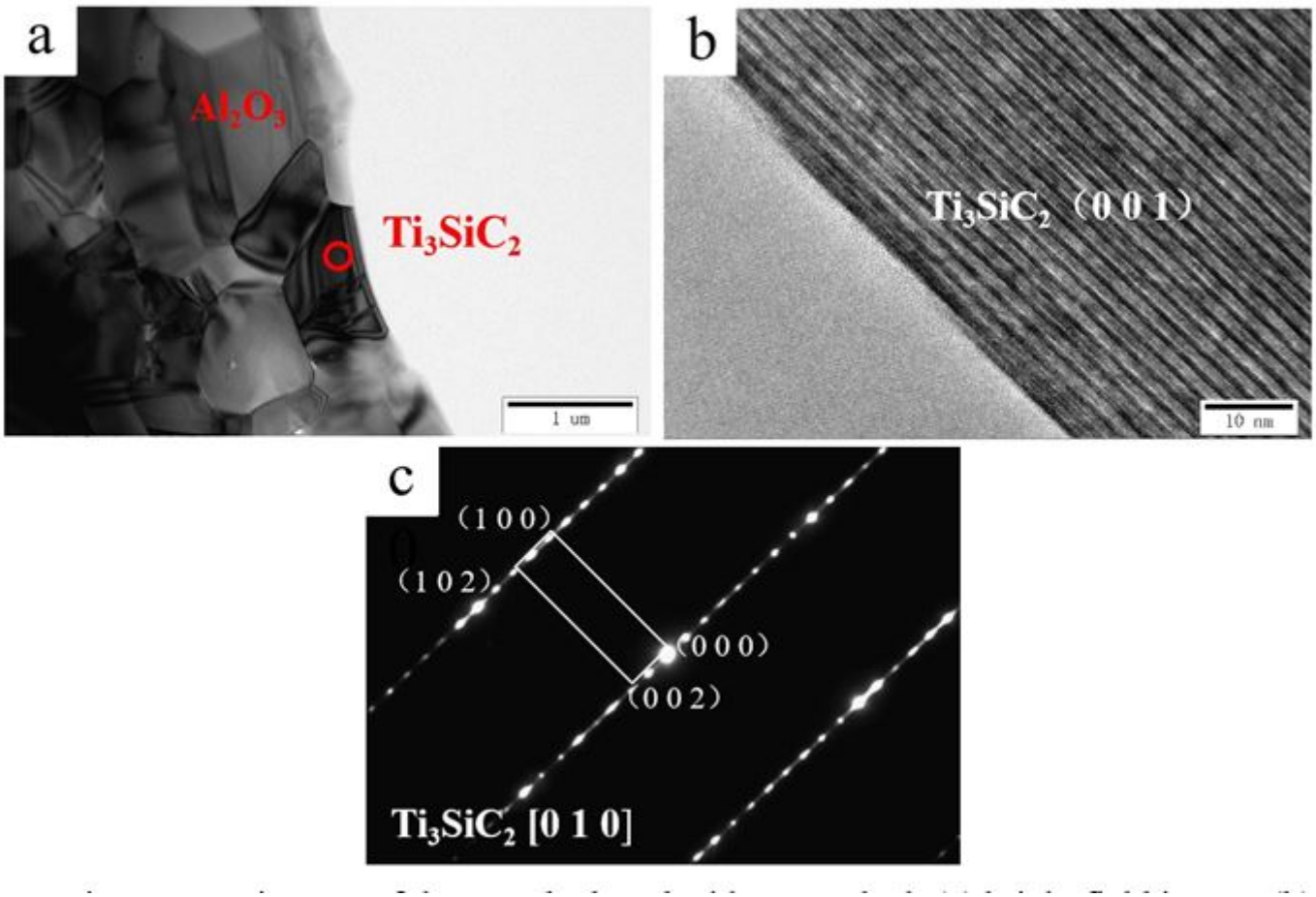

Figure 3

TEM images of the sample doped with 0.2 mol Al: (a) bright field image, (b) HRTEM image, and (c) SAED pattern.

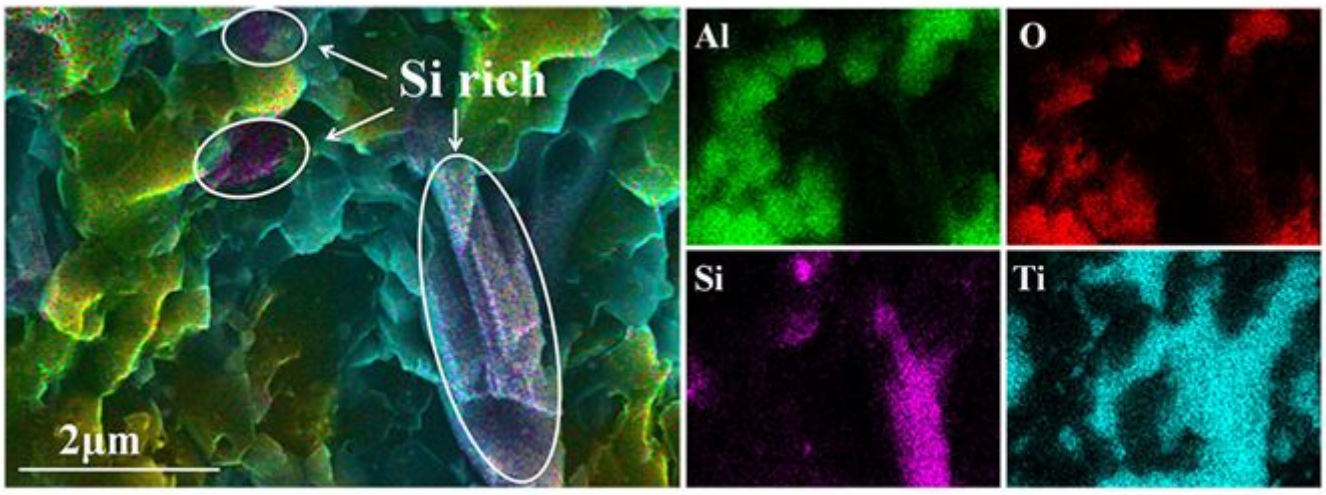

Figure 4

EDS analysis of the sample doped with 0 mol Al.

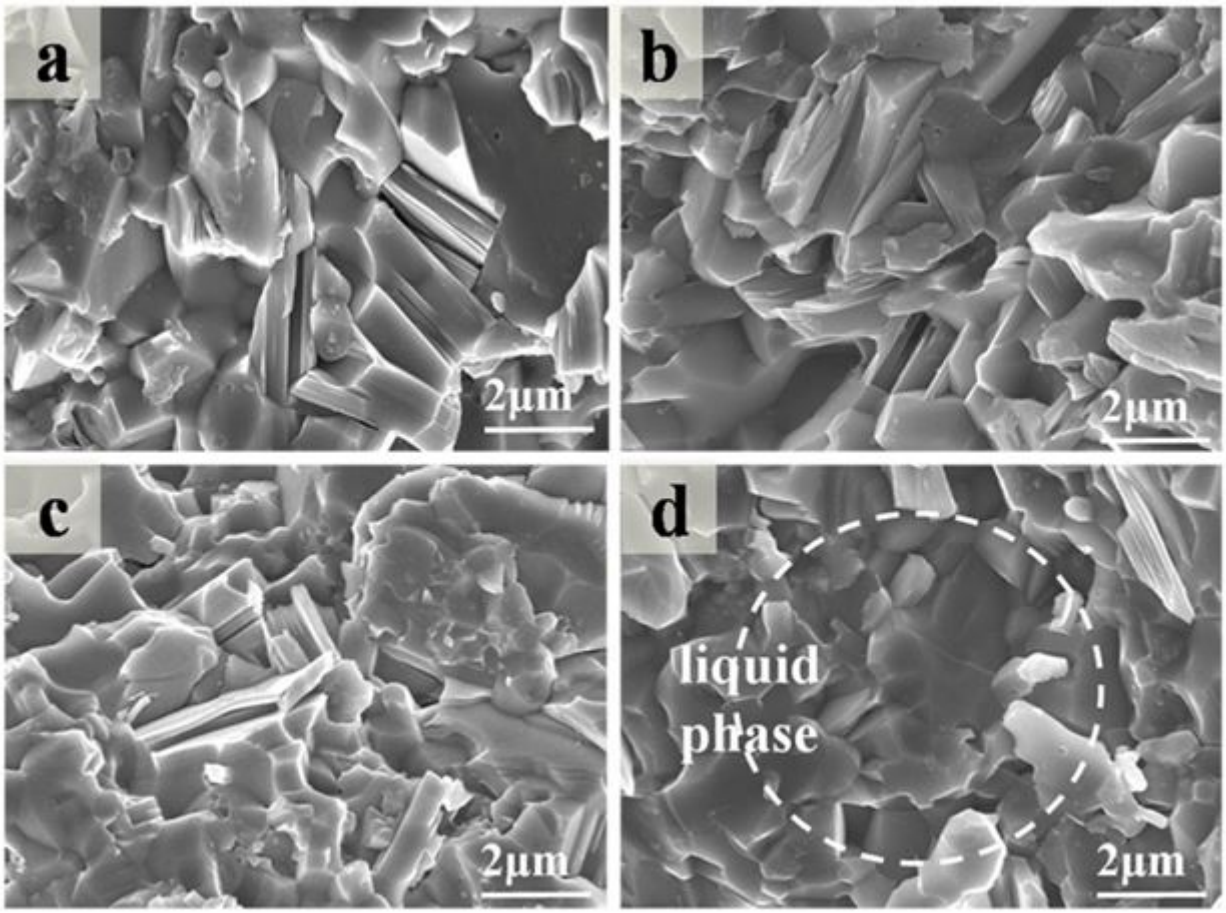

Figure 5

SEM images of the (a) undoped sample and samples doped with (b) 0.1 mol Al, (c) 0.2 mol Al, and (d) 0.25 mol Al.

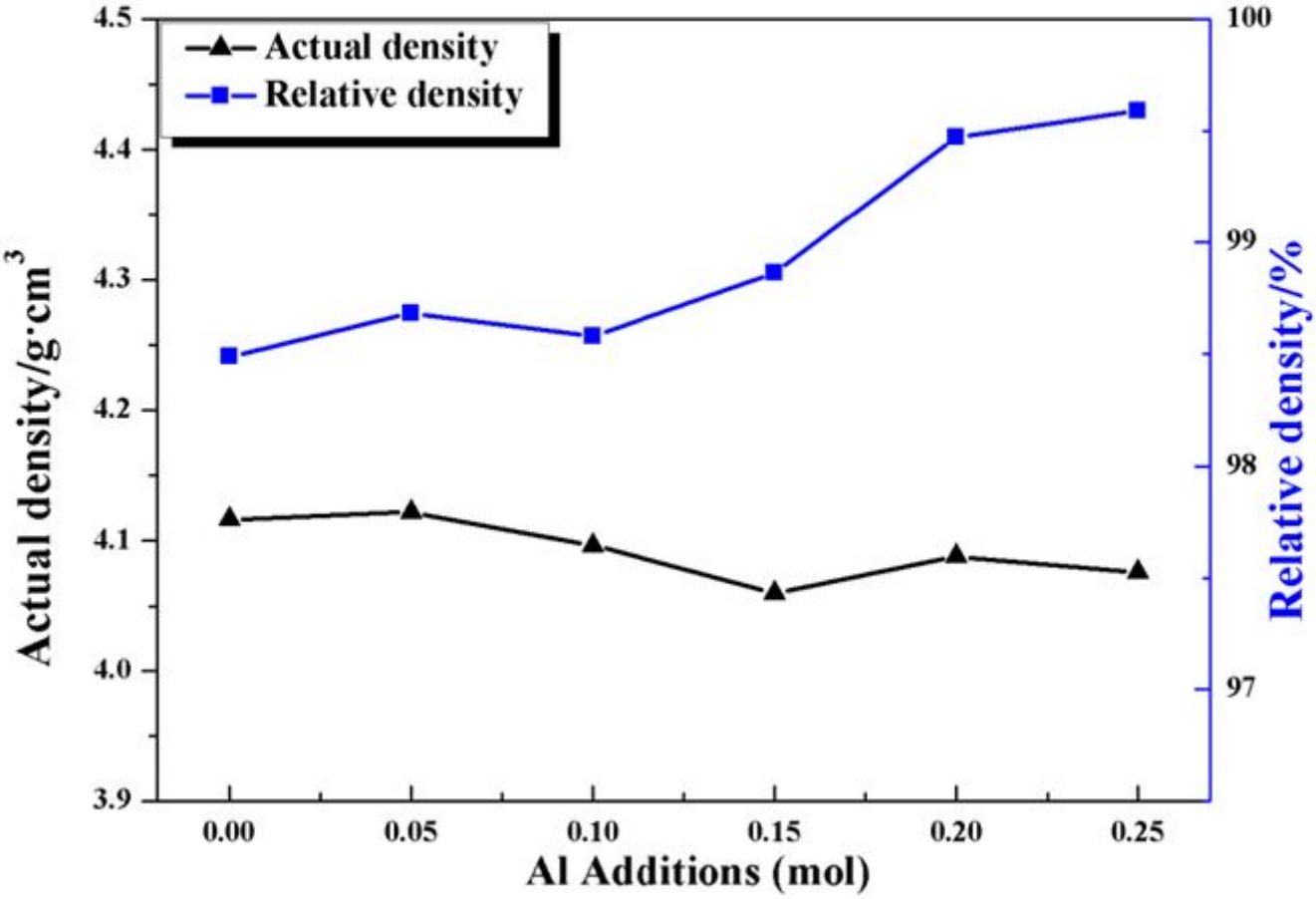

Figure 6

Actual density and relative density of the Ti3SiC2/Al2O3 composites with different Al contents.

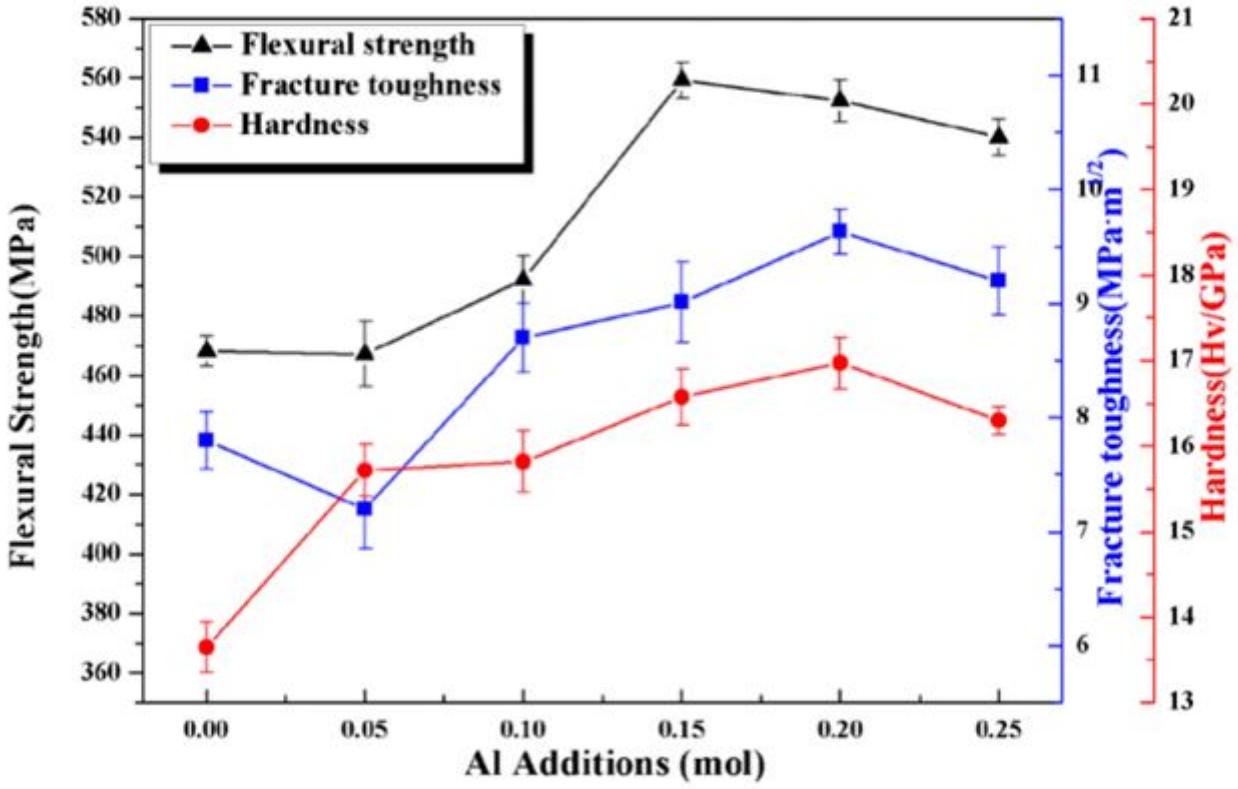

Figure 7

Flexural strength, fracture toughness and hardness of the Ti3SiC2/Al2O3 composites with different Al contents.

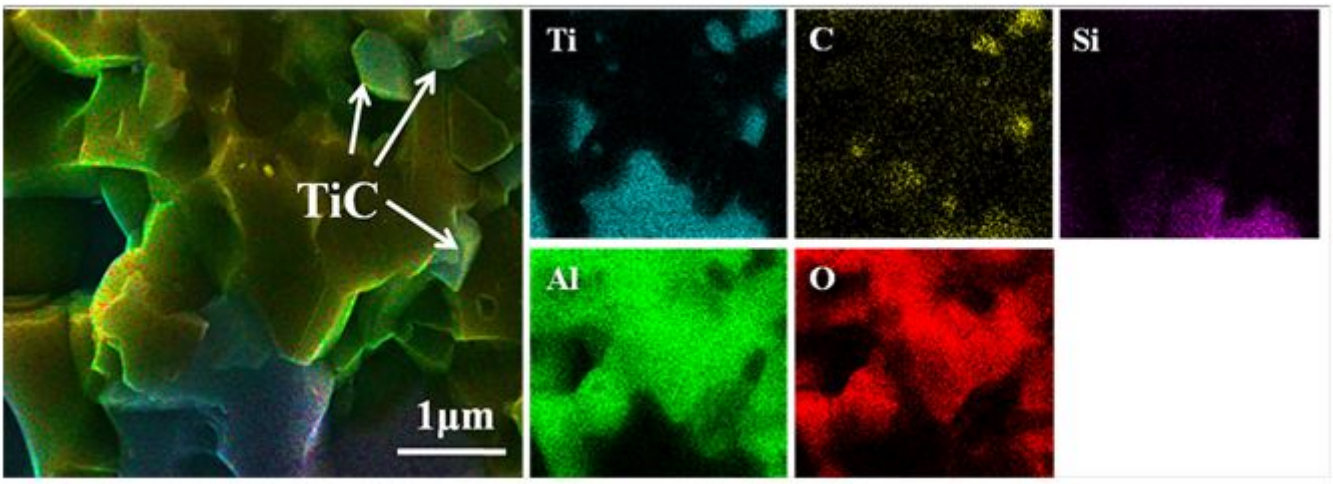

Figure 8

EDS analysis of the sample doped with 0.05 mol Al.

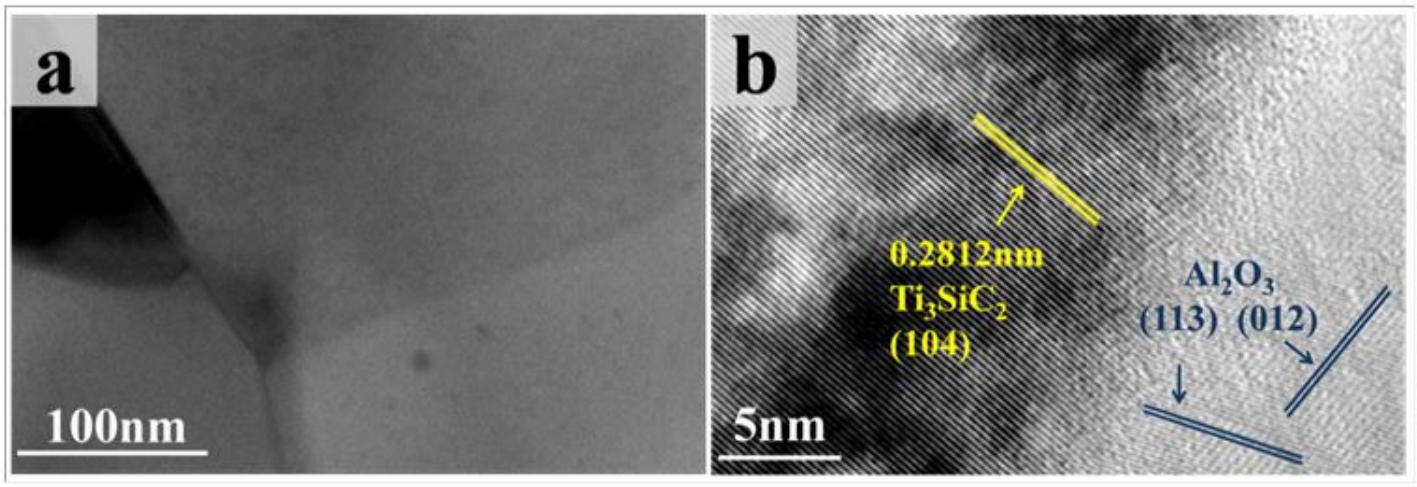

Figure 9

TEM images of the Ti3SiC2 and Al2O3 interface prepared with 0.2 mol Al: (a) bright field image, (b) HRTEM image showing the region between Ti3SiC2 and Al2O3.

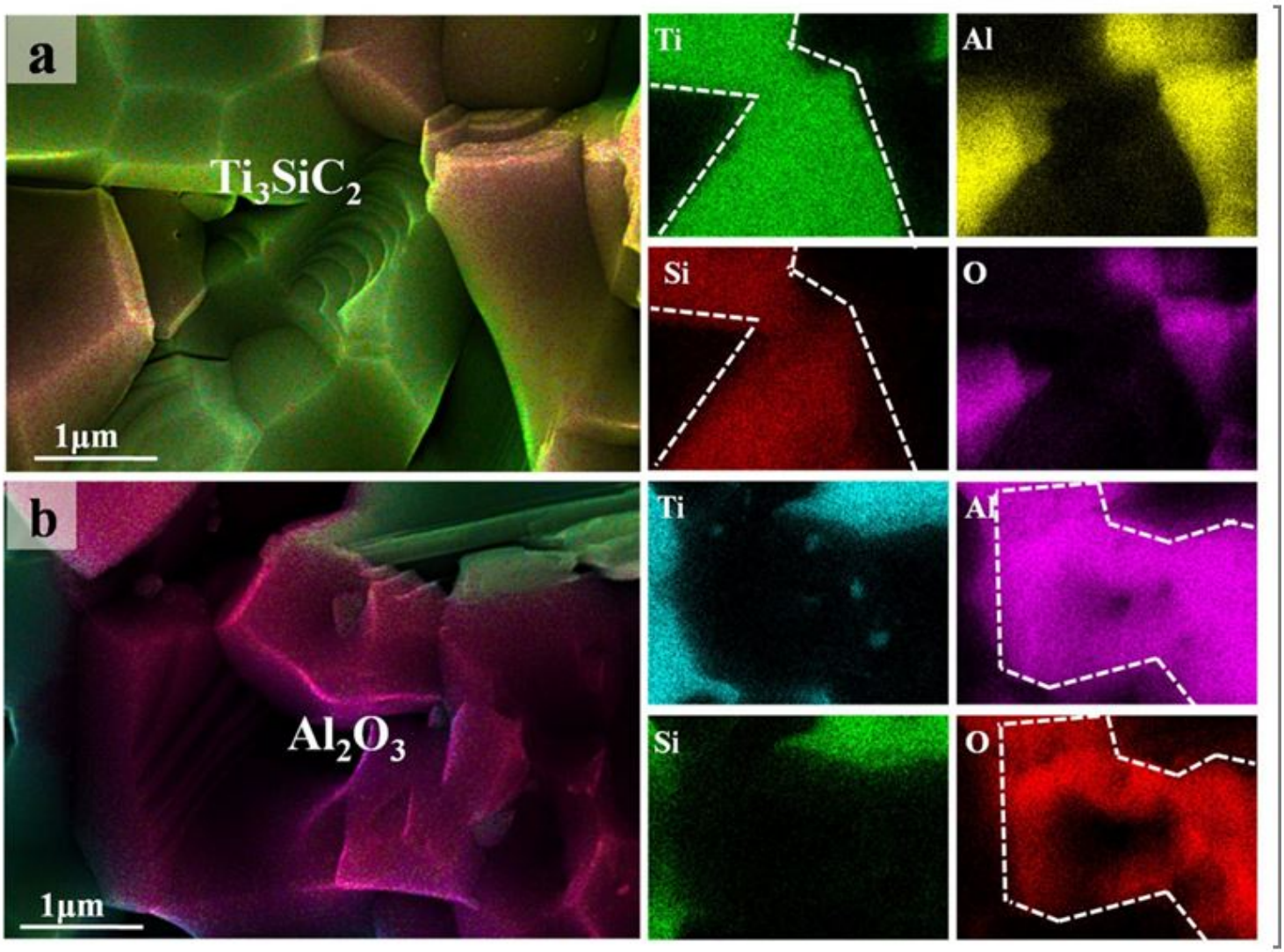

Figure 10

EDS analysis of the sample doped with 0.25 mol Al.

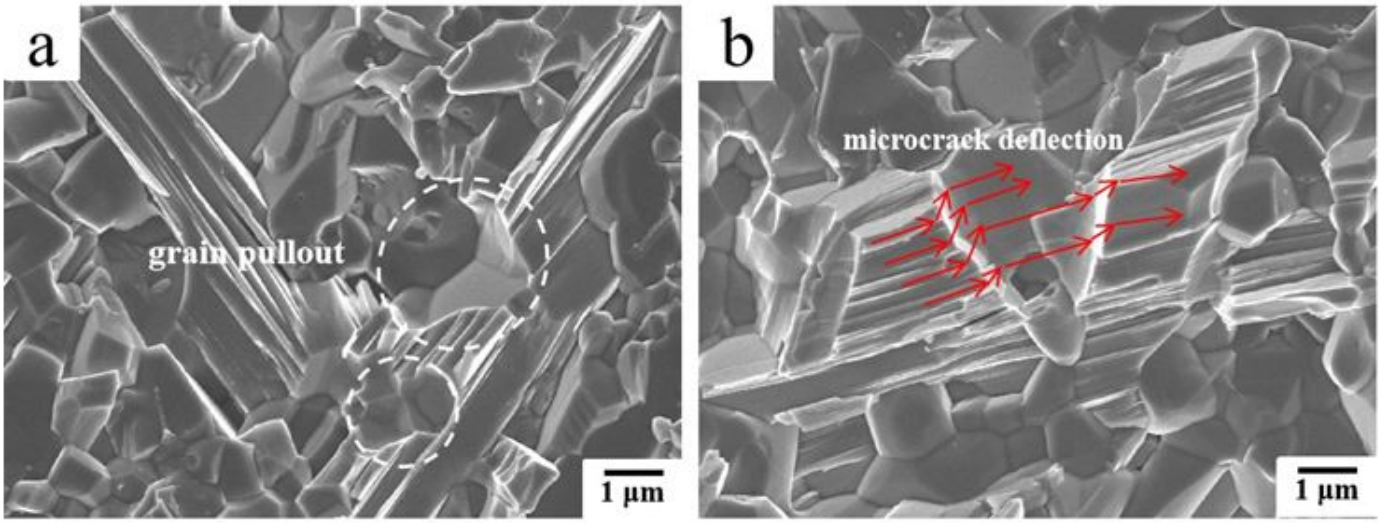

Figure 11

SEM images at high magnification of the sample with 0.2 mol Al.